Available online at www.sciencedirect.com

SciVerse ScienceDirect

Ceramics International 39 (2013) S185–S188

CERAMICS INTERNATIONAL

www.elsevier.com/locate/ceramint

Effects of Cr substitution and oxygen reduction on elastic anomaly and ultrasonic velocity in charge-ordered $Nd_{0.5}Ca_{0.5}Mn_{1-x}Cr_xO_{3-\delta}$ ceramics

S. Shamsuddin, Abdel-Baset M.A. Ibrahim, A.K. Yahya*

Faculty of Applied Sciences, Universiti Teknologi MARA, 40450 Shah Alam, Selangor, Malaysia

Abstract

Charge-ordered $Nd_{0.5}Ca_{0.5}Mn_{1-x}Cr_xO_{3-\delta}$ ceramics have been investigated by electrical resistivity, AC susceptibility and ultrasonic velocity measurements to elucidate the effects of Cr substitution and oxygen reduction on charge ordering (CO). Resistivity and susceptibility measurements showed that the $x=0$ sample exhibits insulating behavior and an anti-ferromagnetic transition at 230 K as well as a CO transition at 280 K. The substitution of Cr induces a ferromagnetic–paramagnetic and metal–insulator (MI) transition as well as gradually suppressing the CO state due to weakening of the Jahn–Teller (JT) effect. Quenching to reduce the oxygen content of the $x=0.05$ sample caused the MI transition temperature to shift to lower temperatures most likely due to oxygen reduction. On the other hand, both longitudinal and shear velocities at 100 K increased significantly with Cr substitution indicating improvement in elastic properties. However, quenching the $x=0.05$ sample slightly deceased both velocities and related elastic moduli. A step-like longitudinal velocity anomaly characterized by a slope change suggests the existence of CO state for $x=0$, 0.02 and 0.05 samples. The step-like anomaly shifts to lower temperatures from 266 K ($x=0$) to 222 K ($x=0.05$) with Cr substitution indicating a weakening of the CO state. Absence of the step-like anomaly for the quenched $x=0.05$ sample suggests suppression of the CO state due to oxygen reduction. Analysis of the step-like anomaly using the mean-field theory suggests involvement of the JT effect which transforms from dynamic to static type with decreasing temperature. Cr substitution weakened the CO state as a result of weakening the JT effect while reducing the oxygen content suppresses the CO state as a result of oxygen reduction.

Keywords: Electrical properties; Magnetic properties; Elastic anomaly

1. Introduction

Hole-doped perovskite manganites with the general formula $Re_{1-x}A_xMnO_3$ (Re = rare-earth, and A = alkaline-earth) have attracted considerable attention due to their Colossal Magnetoresistance (CMR) effect which is commonly attributed to the double-exchange (DE) mechanism [1]. However, studies on these compounds suggested that the CMR effect is also related to the Jahn–Teller (JT) effect [2] and charge-orbital ordering [2]. Usually, the charge ordering (CO) state is often observed in half-doped $Re_{0.5}A_{0.5}MnO_3$(RAMO) perovskite-type manganites in which the ratio of Mn^{3+} and Mn^{4+} is 1:1 and the manganese ions are involved in an order arrangement with localized e_g electrons. Among them, the $Nd_{0.5}Ca_{0.5}MnO_3$(NCMO) has attracted interest due to the existence of CO transition at a higher temperature compared to anti-ferromagnetic (AFM) ordering ($T_{CO} \sim 260$ K, $T_N \sim 160$ K).

Many reports showed that substitution at Mn-sites with a small amount of transition-metal element have influenced the CO state [2,3]. Previous study on $Nd_{0.5}Ca_{0.5}Mn_{1-x}Co_xO_3$ [2] has shown that substitution of Co induces a ferromagnetic–paramagnetic and metal–insulator (MI) transition at low temperature as well as suppresses the CO state. On the other hand, quenching to reduce oxygen content also play a crucial role in influencing the properties of manganites. However, very few reports on effects of reduction in oxygen content on properties of RAMO manganites are available in the literatures [4].

---

*Corresponding author. Tel.: +60 35 5444613; fax: +60 35 5444562.
E-mail address: ahmad191@salam.uitm.edu.my (A.K. Yahya).

0272-8842/$ - see front matter © 2012 Elsevier Ltd and Techna Group S.r.l. All rights reserved.
http://dx.doi.org/10.1016/j.ceramint.2012.10.059

Ultrasonic study at low temperature is useful in providing valuable information on the properties of perovskite manganites [2,6,7]. For example, ultrasonic velocity anomaly has been observed around 250 K for NCMO which indicates transition into CO state and was suggested to be due to strong electron–phonon interaction via the JT effect and substitution of Co at Mn-site of NCMO caused the transition to shift to lower temperatures due to the suppression of the CO state as a result of weakening of the JT effect [2]. However, Cr-doping effect on the CO state in $Nd_{0.5}Ca_{0.5}Mn_{1-x}Cr_xO_{3-\delta}$ (NCMCrO) has not been previously reported. Hence, an ultrasonic study on NCMCrO would be of particular interest to elucidate how Cr substitution and oxygen reduction influenced the CO state as well as providing a better understanding on the role played by the JT effect on CO.

In this paper, we report the effect of Cr doping on ultrasonic, magnetic and transport properties of charge-ordered NCMCrO ceramics. Cr doping has been chosen in this work due to the special nature where Cr^{3+}ion which is iso-electronic in configuration with Mn^{4+}ion. Hence, it is possible that the Cr^{3+} ion may interact with Mn^{3+} ion and induce ferromagnetic-metallic state.

2. Experimental

The NCMCrO ($x=0$, 0.02 and 0.05) samples were synthesized using the standard solid-state reaction method. A stoichiometric mixture of high-purity ($\geq 99.99\%$) Nd_2O_3, CaO, MnO_2 and Cr_2O_3 were ground and calcined at 1000 °C for 24 h with several intermediate grindings. The powders were then pressed and sintered at 1100 °C for 24 h. These samples are now referred as as-prepared samples. The quenched sample was prepared by reheating the $x=0.05$ sample at 1000 °C for 2 h and quenching it directly into liquid nitrogen. Electrical resistivity measurements were carried out using the four-point-probe technique. X-ray powder diffraction showed that all samples were essentially single phased with orthorhombic structure (space group *Pnma*). The AC susceptibility (χ') of the samples was measured using an AC susceptometer system manufactured by CRYO industries, USA with its real component resolved using a 7265 DSP lock-in amplifier. Ultrasonic velocity was measured using Matec 7700 system which utilizes the pulse-echo-overlap technique and performed in a Janis Cryostat Model VNF-100T.

3. Results and discussion

Fig. 1 shows the temperature dependence of electrical resistivity for all samples. The $x=0$ sample showed an insulating behavior but a sharp peak can seen at 280 K for the sample from the $dln\rho/dT^{-1}$ *versus* T curve (inset Fig. 1) indicating the existence of the CO state. However, for the as-prepared $x=0.02$ and 0.05 samples as well as the quenched $x=0.05$ sample no such peak has been observed. This may be an indication that the CO state was weakened by the substitution. A MI transition was observed at around $T_{MI}\sim 133$ K and $T_{MI}\sim 136$ K for the $x=0.02$ and $x=0.05$ samples, respectively. The T_{MI} for the quenched $x=0.05$ sample shifted down to 122 K most likely due to oxygen reduction.

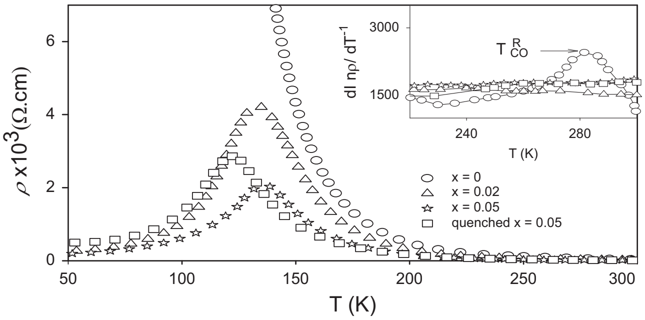

Fig. 1. Temperature dependence of the electrical resistivity of NCMCrO. Inset is the $dln\rho/dT^{-1}$ *versus* T plot.

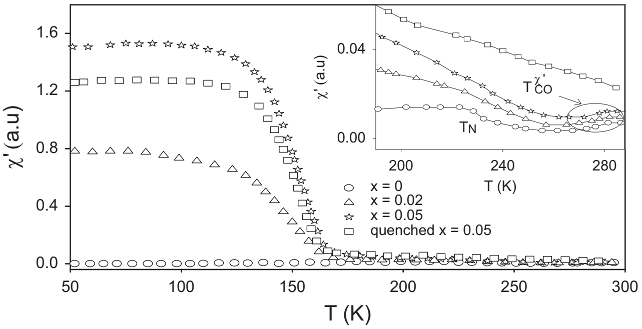

Fig. 2. AC susceptibility *versus* temperature plot for NCMCrO. Inset is an enlarged view of part of the AC susceptibility data.

Fig. 2 shows the results of AC susceptibility (χ') measurements for all samples. The AC susceptibility (χ') data revealed existence of an AFM state with Neel temperature, $T_N\sim 230$ K (inset Fig. 2) for $x=0$. Substitution of Cr induced a FM state with Curie temperature, $T_C\sim 150$ K ($x=0.02$) and $T_C\sim 153$ K ($x=0.05$) clearly showing that the Cr substitutions suppress AFM and promotes the development of FM. This behavior is suggested due to the effect of DE interaction of Mn^{3+}–O–Cr^{3+} [3]. It is possible that Cr^{3+} may play a similar role to Mn^{4+} since Cr^{3+} is a non-JT ion and has the same electronic configuration with Mn^{4+}. At higher temperatures around 280 K, a small drop in χ' indicating a weak AFM transition (inset Fig. 2) which can be associated to a signal of CO transition, T_{co}^{X} was observed for all as-prepared samples. This AFM transition can be related to the existence of the AFM coupling mainly originating from the interaction between Mn^{3+}–O–Mn^{3+} [3]. However, no such transition was observed for quenched $x=0.05$ sample which can be attributed to the suppression of the CO state as a result of oxygen reduction [4].

Table 1 shows the parameters derived from the ultrasonic velocity measurements. The longitudinal and shear modulus are given by $C_l=\rho v_l^2$ and $G=\rho v_s^2$, respectively where ρ is the density, v_l is the longitudinal velocity and

Table 1
Density (ρ), longitudinal velocity (v_l), shear velocity (v_s), longitudinal modulus (C_l), shear modulus (G), bulk modulus (B), Young's modulus (Y) and Debye temperature (θ_D) of NCMCrO.

	Sample			
	$x=0$	$x=0.02$	$x=0.05$	Quenched $x=0.05$
ρ (g/cm^3) ± 0.01	5.19	5.14	5.03	5.02
v_l (km/s) ± 0.01	3.03	3.62	4.12	3.94
v_s (km/s) ± 0.01	2.13	2.54	2.60	2.56
C_l (GPa) ± 0.1	47.6	67.5	85.4	78.0
G (GPa) ± 0.3	23.6	33.1	33.9	32.9
B (GPa) ± 0.5	16.2	23.3	40.2	34.0
Y (GPa) ± 0.3	47.6	67.4	79.4	74.7
θ_D (K) ± 2	266	317	329	323

Sound velocities and related moduli are evaluated at 100 K.

v_s is the shear velocity [5]. The related elastic moduli, bulk modulus (B) and Young's modulus (Y) and acoustic Debye temperature (θ_D) was calculated using the equations below:

$$B = C_l - 4/3G \tag{1}$$

$$Y = 9BG/3B + G \tag{2}$$

$$\theta_D = (h/k_B)(3N/4\pi V)^{1/3} v_m \tag{3}$$

where h is the Planck constant, k_B is the Boltzman constant, N is the number of mass point and V is the unit cell volume calculated from lattice parameter values. The mean velocity, v_m is given by:

$$3/v_m^3 = 1/v_l^3 + 2/v_s^3 \tag{4}$$

The increase in both absolute velocity v_l and v_s with Cr substitution is due to the increase in C_l and G. The behaviors of v_l and v_s can be understood from the equations $v_l = \sqrt{C_l/\rho}$ and $v_s = \sqrt{G/\rho}$ where C_l and G are the independent moduli while both velocities are the dependent variables. Although ρ decreased with Cr substitution, the decrease is less than 1% and it is not suggested to strongly influence the change in both velocities. On the other hand, larger percentage change of 6% and 31% in C_l and G, respectively, is suggested to strongly influence the change in v_l and v_s. Since the velocities were measured at 100 K (Table 1) which is below T_C, the increase of v_l and v_s with Cr substitution is suggested to be due to increase in formation of FM domains which enhances the elastic properties. On the other hand, a small drop in both v_l and v_s at 100 K (Table 1) for the $x=0.05$ sample after quenching can be associated to decrease in C_l and G as a result of oxygen reduction which caused a slightly decreased in FM domain.

Fig. 3. shows the temperature dependencies of the longitudinal and shear velocities for all samples. A step-like longitudinal velocity anomaly characterized by a slope change which can be associated with CO transition signal was observed at T_{co}^{v} for all as-prepared samples. The shifting of the step-like anomalies to lower temperatures with Cr substitution indicates declining of the CO state as the JT effect was weakened. It is possible that, substitution of the Cr^{3+} for Mn^{3+} decreased the ratio of Mn^{3+} to Mn^{4+} and caused the JT effect to weaken and affect the CO state [2]. In the present study, the weakening of the CO state is also supported by the absence of T_{co}^{A} from the resistivity measurements as well as the reduction of χ' around T_{co}^{χ} with Cr^{3+} substitution.

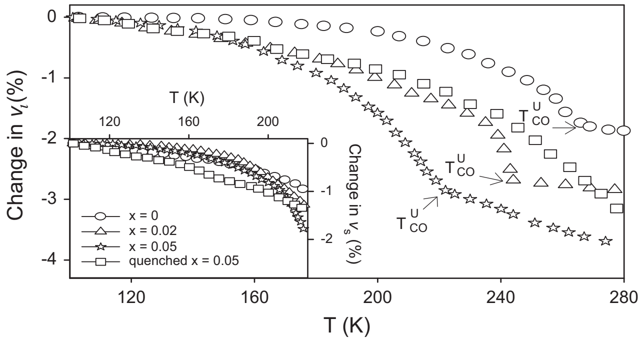

Fig. 3. Temperature dependence of longitudinal velocity in NCMCrO. Inset is temperature *versus* shear velocity in NCMCrO.

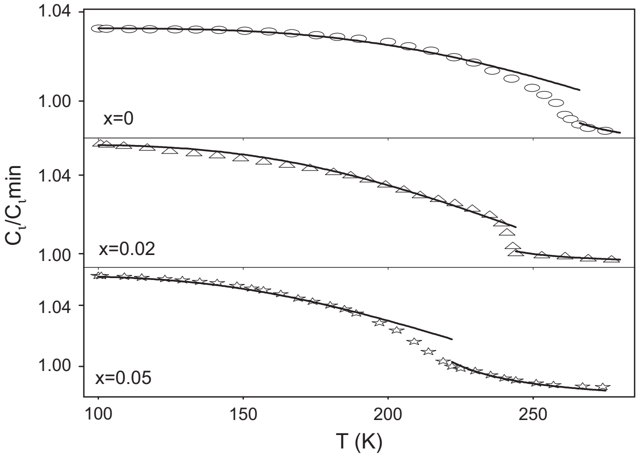

Fig. 4. Temperature dependence of the C_l for NCMCrO. Open symbols are experimental data; solid lines are calculated using Eq. (5) below T_{CO} and Eq. (6) above T_{CO}.

The mean field theory which is related to the JT effect has been used to explain the elastic anomaly occurring in

Table 2
Fitting parameters for C_l using Eq. (5) below T_{CO} and Eq. (6) above T_{CO} for NCMCrO ($0 \le x \le 0.05$).

Sample	T^{v}_{co}(K)	Temp. (K)	$C_0/\ C_{\min}$	$\lambda+\mu$ (meV)	λ (meV)	T^0 (K)	Θ (K)
$x=0$	266	$T<T^{v}_{co}$	1.03	21.80	15.90	–	–
		$T>T^{v}_{co}$	1.06	–	–	233	234
$x=0.02$	244	$T<T^{v}_{co}$	1.06	19.16	13.66	–	–
		$T>T^{v}_{co}$	1.04	–	–	217	218
$x=0.05$	222	$T<T^{v}_{co}$	1.06	17.91	11.86	–	–
		$T>T^{v}_{co}$	1.02	–	–	191	192

the vicinity of the transition temperature in some manganites which is closely related to the strong electron-phonon coupling originating from the JT effect [6,7]. It was suggested that the JT distortion transforms from dynamic type ($T>T_{CO}$) to static-type ($T<T_{CO}$) with decreasing temperature. In the present work the mean field equation was fitted to the temperature dependence of C_l for NCMCrO ($x=0$, 0.02, and 0.05). From the mean field theory, the relationship between the elastic modulus C_l and temperature T below T_{CO} is as follows [7]:

$$\frac{C_l(T)}{C_0}=\left[1-\frac{\lambda+\mu}{k_BT}+\frac{\lambda+\mu}{k_BT}\tanh^2\left(\frac{\Delta}{k_BT}\right)\right] \Big/\left[1-\frac{\lambda}{k_BT}+\frac{\lambda}{k_BT}\tanh^2\left(\frac{\Delta}{k_BT}\right)\right] \quad (5)$$

where C_0 is the longitudinal modulus in the absence of JT coupling, λ is the phonon exchange constant, μ is a measure of the ion-strain coupling and k_B is a Boltzmann constant. The mean filed, Δ is given by $\Delta = k_BT_{CO}\tanh(\Delta/k_BT)$ while, for temperature T above T_{CO} the relationship is written as [7]:

$$C_l(T)/C_0 = T-T^0/T-\Theta \quad (6)$$

where T^0 and Θ are the characteristic temperatures.

From Fig. 4, it can be seen that the fitting results agree well with the experimental data indicating that the JT effect is involved for the CO in NCMCrO ($x=0$, 0.02, and 0.05) which transforms from the dynamic-type ($T>T_{CO}$) to static-type ($T<T_{CO}$) with decreasing temperature. Apart from that, it also can be noticed that the calculated transition temperature [7] $T^{v}_{co}=\lambda+\mu/k_B$ deduced from λ and μ are 253 K, 223 K and 208 K for samples $x=0$, 0.02 and 0.05, respectively, are different compared to the experimental transition temperature, T^{v}_{co} (Table 2). The difference is suggested to be due to the broadening of critical fluctuation of the ion-distortion coupling related to the transition process as suggested from previous report [6]. In addition, the value of λ decreases with Cr content indicating that the electron–phonon interaction weakened in the sample [6].

On the other hand, no longitudinal velocity anomaly was observed for the quenched $x=0.05$ sample. The absence of the longitudinal velocity anomaly for $x=0.05$ sample after quenching could be attributed to the suppression of the CO state as a result of oxygen reduction. It is possible that, due to the quenching effect the oxygen content was reduced causing the Mn^{4+} concentration to decrease and lead to the suppression of the CO state [6]. The suppression of the CO state for the sample is also supported by the absence of both T^{χ}_{co} and T^{A}_{co} in susceptibility and resistivity measurements, respectively.

4. Conclusion

In conclusion, we have systematically investigated the magnetic, transport and elastic properties of charge ordered as-prepared NCMCrO ($x=0$, 0.02, 0.05) and quenched ($x=0.05$) samples. It was found that all as-prepared samples showed a step-like longitudinal velocity anomaly around the vicinity of T_{CO}. Increasing Cr concentration caused the step-like anomaly to shift to lower temperatures indicating that Cr weakened the CO state as a result of weakening of the JT effect. Absence of the step-like anomaly for the quenched $x=0.05$ sample suggests the reduction of the oxygen content effectively suppressed the CO state. On the other hand, Cr substitutions caused the increase in both longitudinal and shear moduli at 100 K indicating improvement in elasticity which is suggested to be due to the increase in FM domain. Quenching the $x=0.05$ sample caused the elastic properties to weaken as a result of reduction in FM domain.

References

[1] C. Zener, Interaction between the d-shells in the transition metal. II. Ferromagnetic compounds of manganese with perovskite structure, Physical Review 82 (1951) 403–405.

[2] Y. Liu, H. Kong, C.F. Zhu, Coexistence of charge ordering and ferromagnetism in $Nd_{0.5}Ca_{0.5}Mn_{1-x}Co_xO_3$ ($x \le 0.1$), Journal of Alloys and Compounds 439 (2007) 33–36.

[3] T. Gao, S. Cao, W. Li, B. Kang, L. Yu, S. Yuan, J. Zhang, Spin glass behavior in the half doped $Pr_{.5}Ca_{0.5}Mn_{1-x}Cr_xO_3$ system, Physica B 404 (2009) 1283–1286.

[4] R. Mahesh, M. Itoh, The effect of oxygen stoichiometry on the structure, magnetism and electron transport properties of the rare earth manganates exhibiting charge ordering, Solid State Ionics 108 (1998) 201–208.

[5] M. Levy, M. Xu, B.K. Sarma, K.J. Sun, Ultrasonic propagation in sintered high-T_C superconductor, in: M. Levy (Ed.), Physical Acoustics (XX) Ultrasonic of High-T_C and other Unconventional Superconductors, Academics Press, New York, 1992, pp. 237–298.

[6] H.D. Zhou, G. Li, H. Chen, R.K. Zheng, X.J. Fan, X.G. Li., The Jahn–Teller effect and electron–phonon interaction in $La_{0.25}Ca_{0.75}Mn_{1-x}Cr_xO_3$, Journal of Physics: Condensed Matter 13 (2001) 6195–6202.

[7] C.X. Chen, J.Y. Zheng, Y.Y. Jiang, J. Li, R.K. Zheng, Elastic anomalies in the perovskite manganite $La_{0.5}Ca_{0.5}MnO_3$, Physica B 405 (2010) 2088–2090.